Available online at www.sciencedirect.com

ScienceDirect

Procedia Structural Integrity 8 (2018) 174–183

Structural Integrity Procedia

www.elsevier.com/locate/procedia

AIAS 2017 International Conference on Stress Analysis, AIAS 2017, 6-9 September 2017, Pisa, Italy

Accelerated cyclic plasticity models for FEM analysis of steelmaking components under thermal loads

J. Srnec Novak[a], L. Moro[a]*, D. Benasciutti[b], F. De Bona[a]

[a] *Politechnic Department of Engineering and Architecture (DPIA), University of Udine, via delle Scienze 208, Udine 33100, Italy*
[b] *Department of Engineering, University of Ferrara, via Saragat 1, 44122, Ferrara, Italy*

Abstract

Steelmaking components are often subjected to thermo-mechanical loads applied cyclically. In this case the choice of a suitable cyclic plastic model to be used in the numerical simulation is a crucial aspect in design. Combined (kinematic and isotropic) model permits the cyclic material behavior to be captured accurately. On the other hand, such model often requires unfeasible computational time to arrive at complete material stabilization. Simplified or accelerated models have then been proposed to make simulation faster. In this work, the thermo-mechanical analysis of a round mold for continuous casting is addressed as a case study. Due to axi-symmetry, a plane model can be adopted. This permits a finite element (FE) analysis with a combined model to be performed until complete stabilization. A comparison with other models able to speed up the simulation (accelerated models with increased values of saturation speed, Prager and stabilized models) was performed. It was found that only accelerated models give equivalent strain range values that do not significantly differ from the (reference) combined model, independently from the speed of saturation adopted.

Peer-review under responsibility of the Scientific Committee of AIAS 2017 International Conference on Stress Analysis

Keywords: cyclic plasticity models; finite element method; thermo-mechanical analysis

* Corresponding author. Tel.: +39 0432 558048
E-mail address: luciano.moro@uniud.it

Peer-review under responsibility of the Scientific Committee of AIAS 2017 International Conference on Stress Analysis
10.1016/j.prostr.2017.12.019

1. Introduction

Frequently steelmaking components undergo thermo-mechanical loads applied cyclically. Typical examples are

Nomenclature

b	speed of stabilization	R_∞	saturation value
b_a	accelerated speed of stabilization	$\boldsymbol{\alpha}'$	back stress deviator tensor
C	initial hardening modulus	γ	nonlinear recovery parameter
C_{lin}	initial hardening modulus (Prager model)	$\Delta\varepsilon_{eq}$	equivalent strain range
E	Young's modulus	$\Delta\varepsilon_{pl}$	plastic strain range
E_s	Young's modulus – stabilized cycle	ε_{pl}	plastic strain
N	number of cycles	$\varepsilon_{pl,acc}$	accumulated plastic strain
N_{stab}	number of cycles to stabilization	$\boldsymbol{\sigma}'$	stress deviator tensor
q	thermal flux	σ_0	initial yield stress
q_{max}	maximum thermal flux	σ_{0*}	actual yield stress
R	drag stress	Δe	relative error

discussed by Srnec Novak at al. (2015), Benasciutti (2012), Benasciutti et al. (2015), Benasciutti et al. (2016), Moro, Benasciutti et al. (2017), for applications spanning from molds for continuous casting to rolls for hot strip rolling and to anodes adopted in electric arc furnaces. All these components operate in contact to steel at high temperature (close to the melting point) and therefore they must be water cooled. It follows that very high thermal gradients occur, producing stresses that frequently exceed yielding. It was recently observed that, in the numerical model adopted to investigate on the mechanical behavior of such components, the choice of the material model could significantly affect the results. As an example, considering a mold for continuous casting, only a combined cyclic plasticity model permits the cyclic material behaviour and permanent distortion, to be simulated accurately, as suggested by Srnec Novak at al. (2015) and Moro, Srnec Novak et al. (2017). As pointed out by Manson (1966), in principle the durability assessment of a component under thermal loads can be performed only if the cyclic behavior is simulated until material stabilization occurs. As materials stabilize approximately at half the number of cycles to failure, it follows that a huge number of cycles must be considered and an unfeasible simulation time would be required by the combined model. Accelerated models have thus been proposed in literature. In particular, in presence of creep and thermal fatigue, authors such as Arya et al. (1990), Dufrenoy and Weichert (2003), Amiable et al. (2006) suggest only a limited number of cycles to be simulated; even if this procedure seems not well defined, it has to be considered that the presence of visco-elasticity generally strongly reduces the stabilization time. If creep constitutes the damage criteria, a more rigorous approach was proposed by Kiewel et al. (2000) and Kontermann et al. (2014), where an extrapolation technique is developed to speed up the simulation. An alternative approach, suggested by Chaboche and Cailletaud (1986) makes use of accelerated models, in particular increasing the value of the parameter b that controls the speed of stabilization in the combined model. Recently, such an approach was adopted by Srnec Novak at al. (2015) to deal with a squared mold for continuous casting. It has been shown that the accelerated model gave the most conservative results, as the lowest value of number of cycles to failure was obtained. On the other hand, the geometry of the squared mold required a 3D FE simulation. Even taking into account symmetries, the number of cycles needed to reach stabilization was approximately 60567 cycles for the considered value of thermal flux, which clearly not permitted simulation to be continued up to complete material stabilization.

In order to validate accelerated models against results from a fully-stabilized simulation, a simpler axi-symmetric round mold is considered in this work as described by Galdiz et al. (2014). Due to axi-simmetry, a plane model can be used and numerical simulations can be performed quite fast until complete material stabilization, which can thus be taken as a reference in the comparison with accelerated models.

2. Cyclic plasticity models

Combined material model (nonlinear kinematic + nonlinear isotropic) is able to capture monotonic elasto-plastic and cyclic hardening/softening behavior of a material. The von Mises yield surface is expressed in Chaboche (2008) as:

$$f = \sqrt{\frac{3}{2}\left(\boldsymbol{\sigma}'-\boldsymbol{\alpha}'\right):\left(\boldsymbol{\sigma}'-\boldsymbol{\alpha}'\right)} - R - \sigma_0 = 0 \tag{1}$$

where $\boldsymbol{\sigma}'$ and $\boldsymbol{\alpha}'$ are the deviatoric stress tensor and the back stress tensor, respectively, R is the drag stress and σ_0 is the initial yield stress. Kinematic part is controlled by $\boldsymbol{\alpha}$ (translation of the yield surface), while isotropic part is related to R, which controls the homothetic expansion of the yield surface during cyclic loading. According to Chaboche (2008), the increment of the back stress, $\mathrm{d}\boldsymbol{\alpha}$, is expressed as a function of the increment of plastic strain, $\mathrm{d}\boldsymbol{\varepsilon}_{\mathrm{pl}}$, and accumulated plastic strain, $\mathrm{d}\varepsilon_{\mathrm{pl,acc}}$:

$$\boldsymbol{\alpha} = \sum_i \boldsymbol{\alpha}_i \quad , \quad \mathrm{d}\boldsymbol{\alpha}_i = \frac{2}{3} C_i \mathrm{d}\boldsymbol{\varepsilon}_{\mathrm{pl}} - \gamma_i \boldsymbol{\alpha}_i \mathrm{d}\varepsilon_{\mathrm{pl,acc}} \tag{2}$$

where C is the initial hardening modulus; the recall parameter γ controls decrease rate of the initial hardening modulus as the plastic strain accumulates. Chaboche model is a superposition of several nonlinear kinematic models. The model with one pair (C_1, γ_1) is known as the Armstrong and Frederick model. Furthermore, considering γ=0 the Prager model (i.e. linear kinematic) is obtained and relation (2) can be expressed as:

$$\mathrm{d}\boldsymbol{\alpha} = \frac{2}{3} C_{\mathrm{lin}} \mathrm{d}\boldsymbol{\varepsilon}_{\mathrm{pl}} \tag{3}$$

Expansion of the yield surface is controlled by the nonlinear isotropic model:

$$\mathrm{d}R = b\left(R_\infty - R\right)\mathrm{d}\varepsilon_{\mathrm{pl,acc}} \tag{4}$$

where b defines the speed of stabilization and R_∞ is the saturation value of the yield surface. R_∞ can be either positive or negative, giving rise to cyclic hardening or softening behavior, respectively. Integration of (4) gives a relationship between R and $\varepsilon_{\mathrm{pl,acc}}$:

$$R = R_\infty \left(1 - e^{-b\varepsilon_{\mathrm{pl,acc}}}\right) \tag{5}$$

A stabilized condition is obtained when R reaches R_∞. Hardening/softening kinetics is mainly governed by the speed of stabilization b and the accumulated plastic strain $\varepsilon_{\mathrm{pl,acc}}$. If the amount of the accumulated plastic strain is relatively small, a huge number of cycles in needed to obtain $R = R_\infty$. Since the accumulated plastic strain depends on loading conditions and cannot be changed, the only available parameter that can be modified to accelerate material stabilization is the speed of stabilization b. Models with increased b parameter, known as “accelerated models”, were firstly introduced in Chaboche and Cailletaud (1986). It was proposed to use a speed of stabilization in the range of (50÷150)b.

3. Thermo-mechanical analysis of the round mold

3.1. Component description

In the continuous casting process, see Fig. 1, molten steel flows from a ladle, through a tundish and thus into the mold, where the liquid steel solidifies against the water-cooled copper walls, to form a solid shell sufficient in strength to contain its liquid core, as explained by Thomas (2001). Downstream of the mold, a further cooling section permits a complete solidification of the steel to be achieved.

The mold is then a key element of the overall process; in fact, it substantially affects the shape and therefore the quality of semi-finished metal casting product. In the case of billets or blooms, the mold is basically a water cooled tube generally with square or round section. The latter case will be studied in this work.

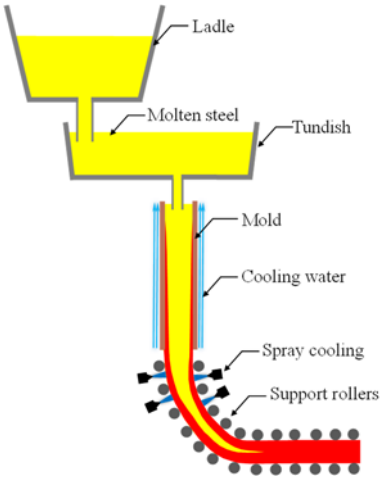

Fig. 1. Schematic description of the continuous casting process of steel.

3.2. Finite element model

A thermo-mechanical analysis of a round mold used in the continuous casting process was performed by means of the finite element method. The analyzed mold is 1000 mm long, with 200 mm inner diameter and 16 mm in thickness, similarly to the case presented by Galdiz (2014). Generally, molds are made of copper alloy in order to achieve high thermal conductivity and good mechanical strength. In this study, a CuAg0.1 alloy was assumed, whose characteristic were experimentally obtained by Srnec Novak (2016). Due to axi-symmetry, a 2D finite element model was adopted, thus strongly decreasing the computational speed. The finite element model has 760 elements and 2487 nodes. The mesh was refined in the meniscus area close to the liquid free surface, see Fig. 3a, where the maximum thermal gradients occur.

3.3. Thermal analysis and results

For the thermal analysis, plane elements with 8 nodes were adopted. A thermal flux was imposed at the inner surface, while convection was considered on the outer surface to simulate water cooling. The thermal flux proposed in Galdiz (2014) was increased of around 50%, to reach a maximum temperature close to 300 °C, for which material parameters are available in Srnec Novak (2016). As a consequence, an increase in the amount of plastic strain was obtained. The temperature of the cooling water is 40 °C and the convection coefficient is 48000 W/m^{2}K. In thermal analysis, the variation of the thermal flux in Fig. 2 was simulated by a sequence of steady state analyses. A nonlinear solution was carried out to simulate the temperature dependence of thermal properties.

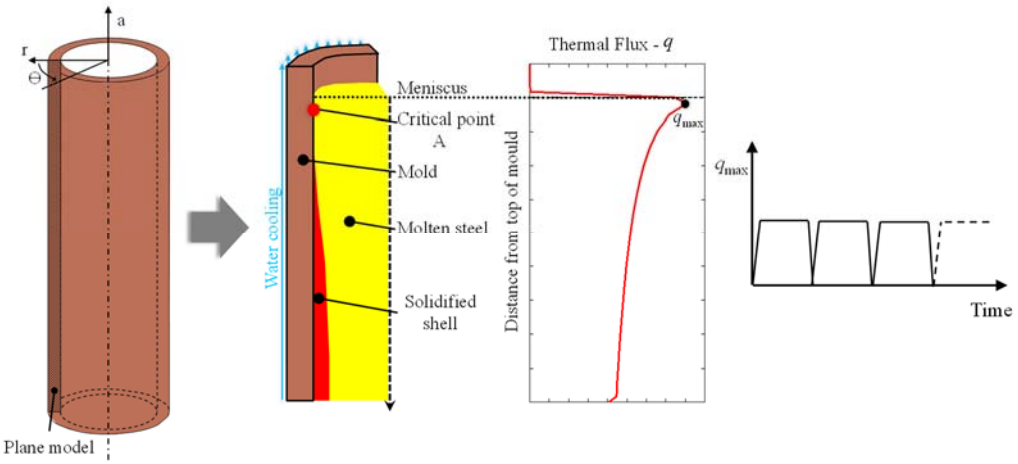

Fig. 2. Schematic description of mold working conditions.

As can be seen in Fig. 3b, the maximum temperatures and thermal gradients occur in the region close to the meniscus. The location of the maximum temperature (298 °C) is labeled with the letter “A”.

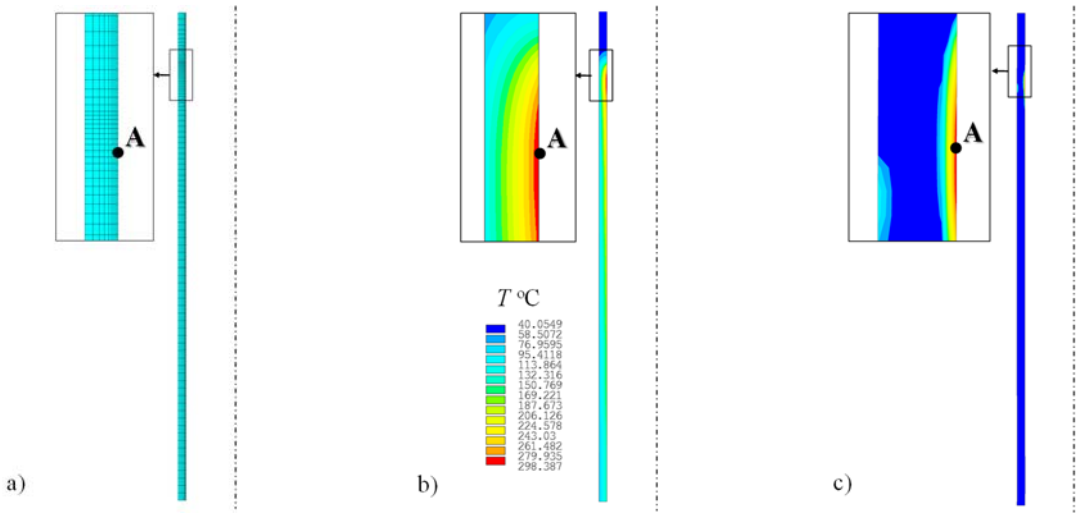

Fig. 3. FEM model a), temperature distribution b), equivalent plastic strain c).

3.4. Mechanical analysis and results

The mechanical analysis was done by imposing as the input data the temperature distribution previously calculated in the thermal analysis. Plane elements with 8 nodes were used. Since the component is free to expand, no mechanical constraints were imposed in the numerical model. Temperature dependence of material parameters was taken into consideration. A combined plasticity model, with parameters taken from Srnec Novak (2016), was used.

The goal of this work is to cyclically load the component until stabilization by using different material models, which are then compared in terms of equivalent strain range, $\Delta\varepsilon_{eq}$. A criterion has to be chosen to establish when material stabilization actually occurs. In this work, it was assumed that material stabilizes when the increment of

maximum von Mises stress was lower than a certain threshold (0.001 MPa in this case). Results obtained with the combined model were compared with those achieved adopting accelerated models with 6 different values of the parameter b_a: 10b, 20b, 30b, 100b, 200b, 300b, covering a wider range with respect to that proposed in Chaboche and Cailletaud (1986). Prager and stabilized models were also implemented for comparison.

Firstly, the combined material model was considered. As proposed by Chaboche (2008), the relation $2bN_{stab}\Delta\varepsilon_{pl}\approx 5$ was used to estimate the number of cycles N_{stab} needed to reach stabilization, $\Delta\varepsilon_{pl}$ being the plastic strain range computed in the first cycles. Considering all three components of plastic strain range ($\Delta\varepsilon_{pl,a}$=0.0004945 axial direction, $\Delta\varepsilon_{pl,\Theta}$=0.0006474 hoop direction and $\Delta\varepsilon_{pl,r}$=0.001145 radial direction) calculated by FE after 10 cycles and assuming $b\approx 5$, it would be necessary to simulate $N_{stab,a}$=1011, $N_{stab,\Theta}$ =772 and $N_{stab,r}$=438 cycles, respectively.

The previous approximate estimations were also confirmed by simulation. As shown in Fig. 4 and Fig. 7, the material stabilizes within 600 cycles. Fig. 4a shows axial, hoop, radial and von Mises maximum stresses at each cycle, versus the number of cycles computed at the critical point A. In this location, a biaxial state of stress occurs, as the radial stress obviously vanishes (free surface). Three components of strain range and the equivalent strain range, evaluated as proposed by Manson (1966),versus the number of cycles are presented in Fig. 4b. It can be observed that the hoop strain range is almost constant, whereas the other two components increase until stabilization. This behaviour can be clearly observed also in Fig. 5, where hoop and axial stress-strain evolution is presented. For the sake of clarity, only the first five cycles, the 200th, the 400th and the final stabilized cycles are presented. The softening phenomenon is more pronounced at the beginning of the cyclic loading, i.e. first five cycles.

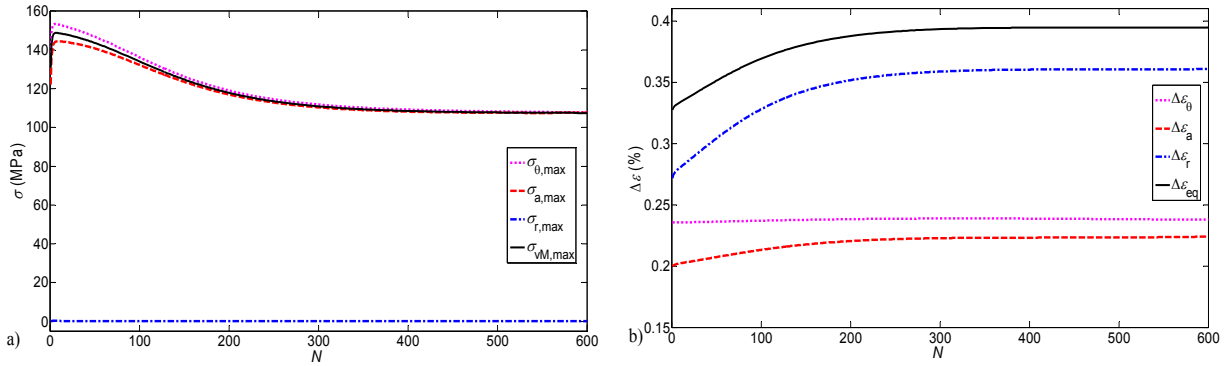

Fig. 4. Maximum stress versus number of cycles a), strain range versus number of cycles b).

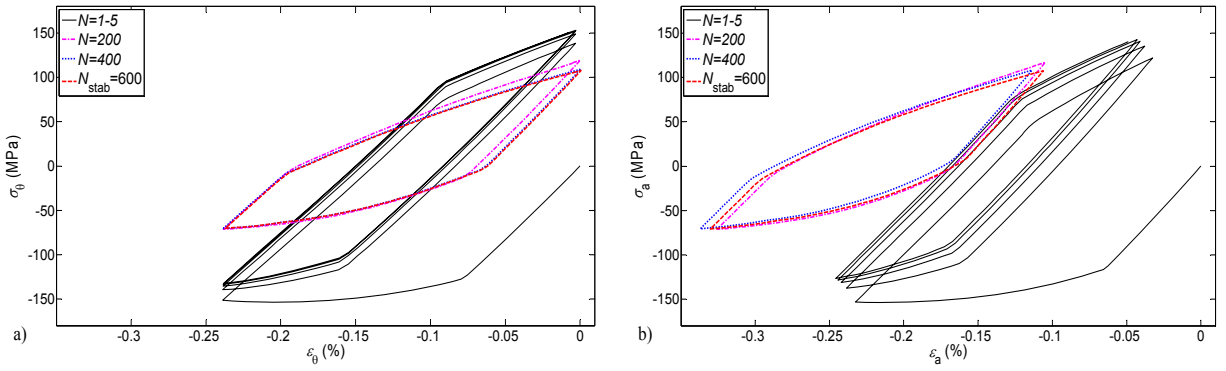

Fig. 5. Combined model - stress-strain loops: hoop direction a), axial direction b).

The results obtained with the accelerated models are now described. Stabilization can be reached faster by increasing the original value of parameter b. The increased speed of stabilization is called b_a (accelerated). In this study, 6 cases with different b_a were studied. In the first case, a value of b_a that is 10 times higher than the original one was considered, then b_a values respectively 20, 30, 100, 200 and 300 times higher were also used. Only hoop stress-strain evolution for the first five cycles and for the stabilized one are presented, see Fig. 6. For low values of b_a (10÷30), see Fig. 6a-c, stress-strain evolution is similar to the combined model. On the other hand, when b_a is high (100÷300), material is forced to stabilize within few cycles; see Fig. 6d-f.

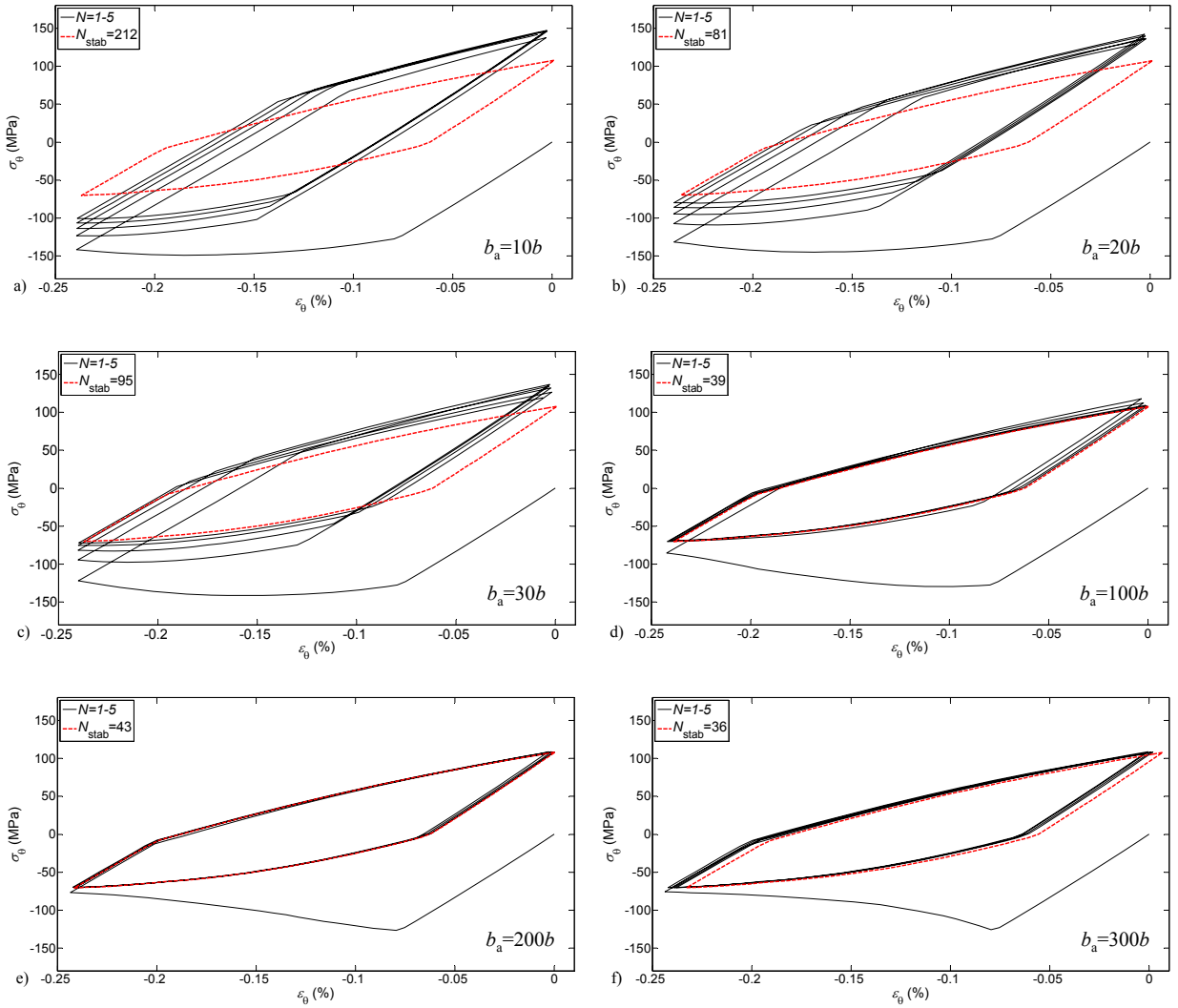

Fig. 6. Hoop stress-strain evolution for different types of accelerated models.

Fig. 7 shows the maximum von Mises stress evolution up to stabilization for the combined and accelerated models. In order to emphasize the differences among the models occurring in first cycles, the N values of each curve are normalized with respect to the corresponding number of cycles to stabilization, N_{stab}. Despite the different values of N_{stab}, the zoom view shows that, at stabilization, all models reach almost the same value of von Mises stress.

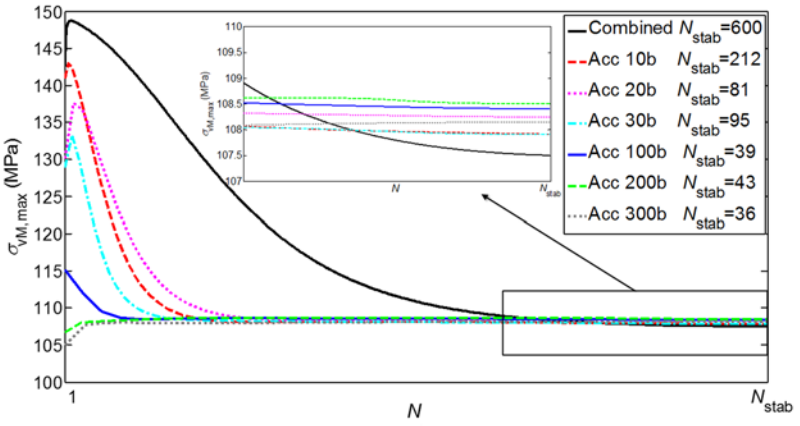

Fig. 7. Maximum von Mises stress evolution up to stabilization.

The equivalent strain range is calculated for 6 different accelerated models and compared with results obtained considering the combined model. In Fig. 8, the evolution of the equivalent strain range from 1st to stabilized cycle is presented. Results obtained with the combined model show a well know "*s-shaped*" curve which corresponds to the adopted nonlinear isotropic model. Quite similar "*s-shaped*" curves are also obtained with the accelerated models with an increased speed of stabilization b_a=10b÷30b, while this shape is lost for higher values of b_a (b_a=100b÷300b), for which, as already shown, the model reaches stabilization almost immediately.

Finally, the Prager and the stabilized models are considered, as they constitute the "limiting" cases corresponding to initial loading and stabilized condition, respectively. Indeed, both approaches are based on kinematic models (linear and nonlinear) and therefore they are able to capture only the monotonic hardening behavior. The Prager model is often proposed in literature because parameter C_{lin} can be estimated by simply using monotonic uniaxial test. The stabilized model, proposed in Chaboche and Cailletaud (1986), supposes that the material is already stabilized at the onset of cyclic loading. Therefore, model parameters E and σ_0 are replaced by E_s and σ_{0*} estimated from stabilized cycles, while kinematic variables (C, γ) remains unaffected.

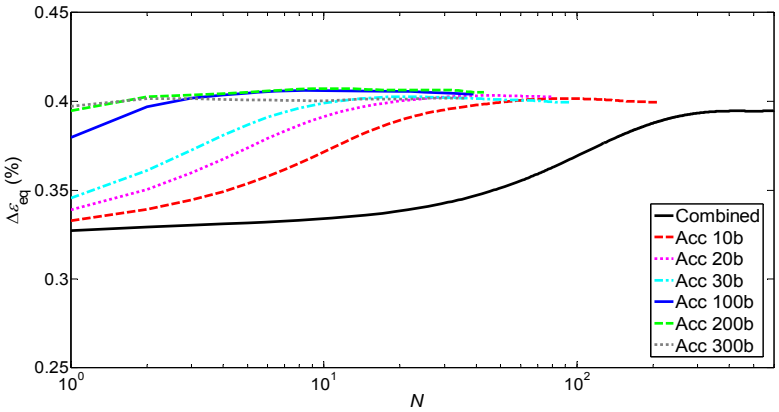

Fig. 8. Equivalent stain range versus number of cycles up to stabilization.

The hoop stress-strain evolution (at the critical point A) calculated with the Prager and the stabilized models are presented in Fig. 9a and 9b. As expected, both models stabilize in few cycles.

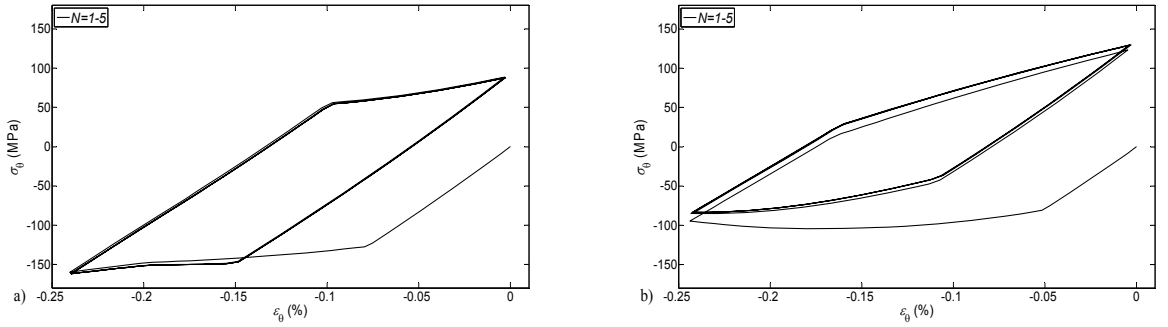

Fig. 9. Hoop stress-strain evolution: Prager model a), Stabilized model b).

The number of cycles to stabilization and the corresponding equivalent strain range are evaluated and listed in Table 1 for all models. As can be noticed, the dependence of $\Delta\varepsilon_{eq}$ on the applied speed of stabilization occurs only in some cases and no marked trend can be identified. Finally, a relative error $\Delta e=(\Delta\varepsilon_{eq,a}-\Delta\varepsilon_{eq,c})/\Delta\varepsilon_{eq,c}$ is calculated where $\Delta\varepsilon_{eq,a}$ and $\Delta\varepsilon_{eq,c}$ are the equivalent strain ranges for the considered accelerated and combined model, respectively. The error remains always in the range 1.16-2.63%. Due to the strong simplification adopted, Prager and stabilized models provide instead a higher relative error (-11.59% and -6.55%). This result is in good agreement with the conclusions in Chaboche and Cailletaud (1986), where it was observed that the direct use of the stabilized model leads to heavy mistakes. As the computation time is almost proportional to the number of cycles to stabilization, it is possible to conclude that the accelerated model permits a strong reduction of the computational effort, keeping the same accuracy as the combined model.

Table 1. Number of cycles to stabilization and equivalent strain range estimated at critical point A.

	Combined model	Accelerated models						Prager model	Stabilized model
		10*b*	20*b*	30*b*	100*b*	200*b*	300*b*		
N_{stab}	600	212	81	95	39	43	36	5	5
$\Delta\varepsilon_{eq}$ (%)	0.3948	0.3994	0.4026	0.3994	0.4041	0.4051	0.4019	0.3490	0.3689
Δe (%)		1.17	1.97	1.16	2.37	2.63	1.8	-11.59	-6.55

4. Conclusions

The choice of the adopted material model in numerical simulations is an important task, particularly when dealing with steelmaking components under cyclic thermo-mechanical loading. Generally, one of the main goals is to capture realistic material behavior; however, very often, this requires complex and sophisticated models. Moreover, sometimes stabilized condition cannot be achieved even with the most suitable model because unfeasible computational time is required. Some alternative models have been thus proposed in literature. In this work, several models (combined, accelerated, Prager and stabilized models) have been considered and compared in terms of equivalent strain range. Based on the obtained results, it is possible to conclude that the use of too simplified models (Prager and stabilized) neglecting initial or stabilized conditions may be dangerous, as they could provide inaccurate cyclic material behavior. On the other hand, accelerated models give results that are always close to the fully-stabilized combined model, assumed as reference. It seems possible to conclude that when dealing with components with a more complex geometry than the round mold studied in this work, the choice of b_a parameter must be carefully set up to get a feasible computational time.

References

Amiable, S., Chapuliot, S., Constantinescu, A., Fissolo, A., 2006. A Computational Lifetime Prediction of a Thermal Shock Experiment. Part I: Thermomechanical Modelling and Lifetime Prediction, Fatigue & Fracture of Engineering Materials & Structures 29, 209-217.

Arya, V.K., Melis, M.E., Halford, G.R., 1990. Finite Element Elastic-Plastic-Creep and Cyclic Life Analysis of a Cowl Lip, NASA Technical Memoranudm, 102342.

Benasciutti, D., 2012. On Thermal Stress and Fatigue Life Evaluation in Work Rolls of Hot Rolling Mill, Journal of Strain Analysis for Engineering Design 47(5), 297-312.

Benasciutti, D., De Bona, F. and Munteanu, M.Gh. 2015. An Harmonic 1D-element for Non linear Analysis of Axisymmetric Structures: The Case of Hot Rolling, Proc. of 1st Pan-American Congress on Computational Mechanics (PANACM 2015) and 11th Argentine Congress on Computational Mechanics (MECOM 2015), Buenos Aires, 27-29 April 2015, 1566-1577.

Benasciutti, D., De Bona, F. and Munteanu, M.Gh., 2016. A Harmonic One-dimensional Element for Non-linear Thermo-Mechanical Analysis of Axisymmetric Structures under Asymmetric loads: The Case of Hot Strip Rolling, Journal of Strain Analysis for Engineering Design 51(7), 518-531.

Chaboche, J.L., 2008. A Review of Some Plasticity and Viscoplasticity Constitutive Theories, International Journal of Plasticity 24, 1642-1693.

Chaboche, J.L., Cailletaud, G., 1986. On the Calculation of Structures in Cyclic Plasticity or Viscoplasticity, Computers & Structures 23, 23-31.

Dufrenoy, P., Weichert, D., 2003. A Thermomechanical Model for the Analysis of Disc Brake Fracture Mechanisms, Journal of Thermal Stresses 26, 815-828.

Galdiz, P., Palacios, J., Arana, J.L., Thomas, B.G., 2014. Round Continuous Casting with EMS-CFD Coupled, European Continuous Casting Conference, Graz, Austria.

Kiewel, H., Aktaa, J., Munz, D., 2000. Application of an Extrapolation Method in Thermocyclic Failure Analysis, Computer Methods in Applied Mechanics and Engineering 182, 55-71.

Kontermann, C., Scholz, A., Oechsner, M., 2014. A Method to Reduce Calculation Time for FE Simulations Using Constitutive Material Models, Materials at High Temperatures 31, 334-342.

Manson, S. S. 1966. Thermal Stress and Low-Cycle Fatigue, McGraw-Hill book company.

Moro, L. Srnec Novak, J., Benasciutti, D., De Bona, F. 2017. Copper Mold for Continuous Casting of Steel: Modelling Strategies to Assess Thermal Distortion and Durability. Key Engineering Materials 754, 287-290, (doi:10.4028/www.scientific.net/KEM.754.287).

Moro, L., Benasciutti, D., De Bona, F. and Munteanu, M.Gh. 2017 Simplified Numerical Approach for the Thermo-Mechanical Analysis of Steelmaking Components under Cyclic Loading: An Anode for Electric Arc Furnace, Ironmaking and Steelmaking, published on line (doi: 10.1080/03019233.2017.1339482).

Srnec Novak, J., Benasciutti, D., De Bona, F., Stanojevic, Huter, P., 2015. Thermo-mechanical Finite Element Simulation and Fatigue Life Assessment of a Copper Mould for Continuous Casting of Steel, Procedia Engineering 133, 688-697.

Srnec Novak, J., Benasciutti, D., De Bona, F., Stanojevic, A., De Luca, A. and Raffaglio, Y., 2016. Estimation of Material Parameters in Nonlinear Hardening Plasticity Models and Strain Life Curves for CuAg alloy. IOP Conf. Series: Materials Science and Engineering, 119, 012020.

Thomas, B.G., 2001. Continuous Casting of Steel. Chapter 15 in Modeling for Casting and Solidification Processing, Dekker, M. (Ed.), New York, 499-540.